

Automatic Coronary Calcium Scoring using Computed Tomography

Didi de Gouw
Utrecht University 2014

Abstract – Coronary calcium is a significant predictor for atherosclerosis and future cardiovascular events. The manual approach for coronary calcium scoring is intensive and time-consuming. Different methods have been developed to automate this task. Coronary calcium is currently scored on non-contrast ECG-synchronized coronary computed tomography (CT), but can be scored with different CT scan techniques. This thesis will give an overview of methods for automatic calcium scoring. Several fully automatic and semi-automatic methods are discussed with the used scan techniques and mutually compared.

1. Introduction

Coronary artery disease (CAD) is one of the leading causes of mortality worldwide¹. Early detection and quantification of coronary plaques is therefore of high interest. Different studies have shown that coronary calcium is a significant predictor of atherosclerosis disease and correlates with the risk for future cardiovascular events^{1,2,3,4}. Specially, the absence of calcium shows an excellent negative predictive value for cardiac events⁴. Observing the change in calcium score also makes it possible to assess the progression of CAD and monitor the efficacy of medical therapies⁵.

Coronary calcium can be located in any of the two main coronary arteries and their sub branches: left main (LM), left anterior descending (LAD), left circumflex (LCX), right coronary artery (RCA), and posterior descending (PDA)⁴. This can be visualized with different modalities. A commonly used modality for the detection and quantification of coronary calcium is Computed Tomography (CT). CT is, apart from the radiation, a non-invasive technique and the calcium score is comparable with the reference technique for the evaluation a coronary plaque, Intravascular Ultrasound (IVUS)⁴. This thesis will focus on calcium scoring using CT only.

The standard scanning protocol for evaluation of CAD consists of two CT scans. First, a low resolution unenhanced coronary CT with ECG-synchronization (CT) is used to determine the calcium score. Secondly, a contrast enhanced coronary CT (CTA) is made. This scan visualizes morphology of the vessel lumen and is mainly used for evaluation of soft plaques³. Coronary calcifications are visualized as highly dense regions

compared to soft tissues on CT. A radiologist has to manually identify all calcifications, which is an intensive and time-consuming task. This can be prevented, by automatically calculating the coronary calcium score and cardiovascular risk⁶.

In this thesis, different ways to automatically determine the calcium score will be discussed. The advantages and disadvantages will be described and the different methods will be mutually compared. First the different scores for coronary calcium and risk assessment will be discussed. The different calcium scores are important for the evaluation of the different automatic methods. The automatic scoring methods are based on different scan techniques. Therefore, the different scan techniques will be briefly explained before the automatic methods are discussed.

2. Manual calcium score and risk assessment

In current clinical practice, the total coronary calcium score and corresponding cardiac risk is semi-automatically quantified. For the evaluation of coronary calcium there are three different calcium scores, the Agatston⁷, volume⁸ and mass score⁹.

2.1.1 Agatston score

The score introduced by Agatston⁷ is based on electron beam computed tomography (EBCT) with a slice thickness of 3 mm and non-overlapping slices. In this 2D method coronary calcium is defined as an area of at least 1 mm² with a density above a threshold of 130 Hounsfield units (HU), three standard deviations above the heart mean-soft-tissue attenuation of the heart. The minimum value of 1 mm² is for eliminating noise. For every calcified lesion, the area (A) and weighting factor (W) are defined per slice. The weighting factor of the lesion per slice is defined by the maximum intensity value, I of the calcification in the follow manner:

$$\begin{aligned} 1 &= 130 \text{ HU} \geq I \leq 199 \text{ HU} \\ 2 &= 200 \text{ HU} \geq I \leq 299 \text{ HU} \\ 3 &= 300 \text{ HU} \geq I \leq 399 \text{ HU} \\ 4 &= I \geq 400 \text{ HU} \end{aligned}$$

The score for one lesion is then calculated by summing the scores of all the slices of the lesion. The Agatston score, AS for a calcification is therefore given by:

$$AS\ object = \sum_{i=1}^n A_i * W_i$$

Where A_i and W_i are the area and weighting factor of the lesion for the respective slice i and n the total number of slices of the object. The total Agatston score is then the sum of all calcifications in the coronary arteries in the scan. The Agatston score is based on EBCT. However, the results of EBCT in coronary calcium score are comparable with MDCT¹⁰. Therefore the Agatston score method can also be used for MDCT. The Agatston score is a widely used scoring method and largely accepted⁴. However, this scoring method is not always accurate and reproducible. This is mainly because the weighting factor is based on the peak calcium attenuation value⁹.

2.1.2 Volume score

Another scoring method is the volume score method⁸. This is an isotropic interpolation method. The number of voxels >130 HU are multiplied with the voxel volume using isotropic interpolation. Compared with the Agatston score, the volume score is better reproducible¹¹. However, this method is not adequate to compare calcium score using different CT protocols and scanners. Due to the partial volume artefact, the method will overestimate the calcium volume of big lesions and underestimate small lesions⁴.

2.1.3 Mass score

A third algorithm, the mass score, measures the mineral content of calcified plaques⁹. This score method requires scanner and scan protocol calibration of the CT attenuation using a reference calcium hydroxyapatite phantom. First, the calcium concentration is calculated as the mean CT attenuation for all voxels in a calcified lesion. The mean calcium concentration is then derived from the association between the calculated mean attenuation and the calcium concentration in the calibration phantom. To calculate the mineral mass per plaque, the calcium concentration is multiplied by the volume of the calcified plaque. The total mass score is then the sum of all calcified plaques¹¹. The mass score is more accurate and less variable than the Agatston or volume method and recently preferred by a group of experts. Because the volume and mass score are both hindered by limited registry data, the widely used score is still the Agatston score⁴.

2.3 Risk classification

A risk prediction of future cardiac events can be made with the calcium score. All calcium scores result in the same accuracy in risk stratification⁴. For the Agatston score standardized categories for the cardiovascular risk have been developed¹². This risk is given by:

1. low risk = $0 \geq As \leq 10$
2. moderate risk = $11 \geq As \leq 100$
3. high risk = $101 \geq As \leq 400$
4. very high risk = $As \geq 400$

The calcium score can also be added to a prediction model based on traditional risk factors, such as age, blood pressure, and tobacco use². With this prediction model the classification of risk significantly improves and places more individuals in the most extreme risk category^{2,13}.

3. Calcium scoring in different scan-techniques

The calcium score is usually determined with CT, although this is possible with any CT scan that visualizes the heart¹⁴. Different automatic and non-automatic studies are performed with EBCT, CT, CTA and low dose chest CT. The used scan technique is important to mutually compare the different automatic methods. In the next section, the different scan techniques will be briefly explained.

3.1 EBCT

Before the introduction of multi detector computer tomography (MDCT), the only tomographic scanner capable of noninvasively visualizing the coronary arteries was EBCT. EBCT is an especially fast form of x-ray imaging technology. A stationary source-detector combination and a rotating electron beam are used to detect and measure calcium deposits in the coronary arteries¹⁵. EBCT is a fast and safe examination, it does not use contrast agents and has a low radiation dose of approximately 1 mSv. The low radiation dose is due to prospective ECG triggering. A high energy beam is produced in the mid-end diastole, where there is less influence of cardiac motion. The disadvantages of EBCT are the poor spatial resolution and the impossibility of performing angiographic scans⁴. For the manual calcium score, all scoring methods in 2.1 can be used. In non-contrast enhanced scans, coronary arteries are not visible unless they are calcified or embedded in fat. Consequently, automatic segmentation of coronary arteries is not possible. The coronary calcifications appear as high-density structures in the EBCT scans, However, it is difficult to identify them automatically, because the

presence of other similar high-density structures, including the non-coronary calcifications⁶.

3.2 CT

Currently, calcium scoring is performed on non-contrast CT scans. MDCT allows image reconstruction with a small section increment and thus improves the reproducibility of the calcium score. In CT scans the same problem as in EBCT occurs, with the low contrast between the coronary arteries and surrounding tissue, it is very difficult to accurately segment the coronary arteries. An advantage of this scan technique is that a low radiation dose is used. However, this low dose leads to noise, which makes it even harder to discriminate between coronary calcium and surrounding tissue. Furthermore, despite the ECG synchronization techniques, motion artefacts may occur. This can cause blurring of the coronary arteries so that calcifications are not visible anymore¹⁶.

3.3 CTA

It is common practice today to perform a calcium scoring CS study followed by a CTA. A high calcium score used to be a contra-indication for CTA, because the CT scanners were unable to perform a diagnostic quality scan with heavily calcified coronary arteries. Nowadays, with the new generation of CT scanners, this is no longer a contra-indication¹⁷. If the coronary calcium can be quantified on CTA, only one CT scan has to be made, which reduces the overall radiation dose and discomfort for the patient. Vessels containing contrast agent are relatively homogeneous and have a high contrast with respect to the surrounding tissue. For the quantification it is hard to find a good threshold, because it needs to be high enough to not misinterpret intravascular contrast medium and image noise as calcification and low enough, so that calcified plaques are not missed^{18,19}.

3.4 Chest CT

In the screening trials for heavy smokers a low dose chest CT without ECG-synchronization is made. Researchers found that heavy smokers that

are screened for lung cancer also have a high risk for cardiovascular events²⁰. Therefore, it is advantageous to screen for the CAD and lung cancer simultaneously in the chest CT scan. However, with low radiation dose and without ECG-synchronization, there is a lot of image noise and cardiac motion, which makes quantification of coronary calcium very hard. Nowadays, with MDCT scanners it is possible to have faster gantry rotation times, thinner slices and more detector rows, which will reduce susceptibility to cardiac motion and partial volume effects²¹. In chest CT a large field of view (FOV) is applied with thin slices. To reduce image noise and improve the detection of coronary calcifications, an additional dataset should be reconstructed, using a small FOV and thicker slice^{12,22,23}. A recent study with 50 COPD patients showed a very strong correlation (0.96) between cardiac CT and chest CT in determining the calcium score²¹. Moreover, no patient who had coronary artery calcium on cardiac CT scans had a zero calcium score in chest CT scans. Furthermore, other studies with smokers and non-smokers show similar results for the coronary calcium score^{20,23}.

4. Automatic calcium scoring methods

In this next section different automatic calcium scoring methods will be discussed. The automatic calcium scoring methods are organized per different scan technique because in every scan technique, the representation of the coronary arteries, calcium and other structures can be different. This will lead to different methods to subtract coronary calcium. Therefore, organizing the automatic methods by scan technique will make for better comparison (fig 1).

An automatic method can be evaluated on several criteria. Most automatic methods are compared with the manual coronary calcium scoring performed by an expert. The three most important criteria are sensitivity, specificity and accuracy. These statistical performance measures can be computed in terms of true-positives (TP), true-negatives (TN), false-positives (FP) and false-negatives (FN) as followed:

$$\text{Sensitivity} = \frac{TP}{TP+FN}$$

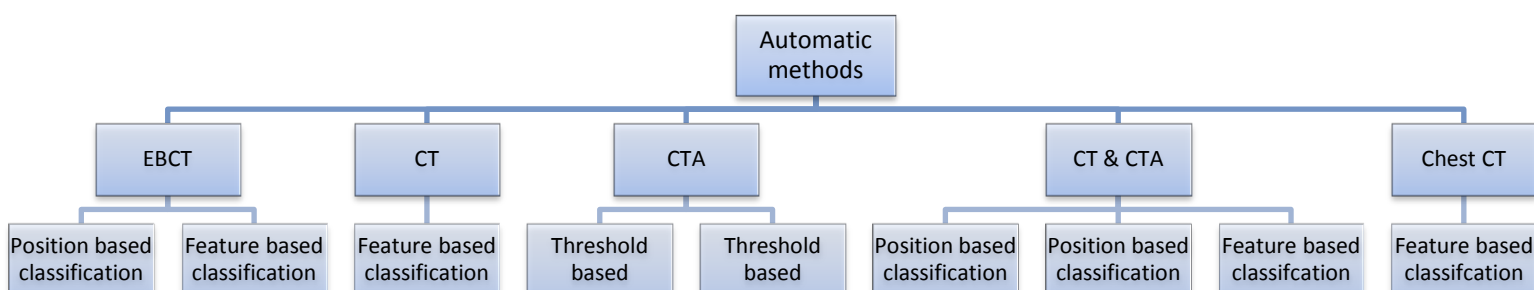


Figure 1: Overview of the subdivisions of the automatic calcium score methods

$$\text{Specificity} = \frac{\text{TN}}{\text{TN} + \text{FP}}$$

$$\text{Accuracy} = \frac{\text{TP} + \text{TN}}{\text{TP} + \text{TN} + \text{FP} + \text{FN}}$$

Another important criterion is the risk classification. This is important because the calcium score is calculated to predict the cardiac risk for a patient. However, only a few of the automatic methods used this for the evaluation of the method.

4.1 EBCT

To identify a coronary calcification among the candidate regions, a human observer mostly relies on prior knowledge of the expected location of the coronary arteries relative to the heart. Therefore both methods^{6,24} for automatic calcium scoring in EBCT make use of a heart-centered coordinate system (HCCS). There are different techniques for constructing a HCCS. One method, described by Brunner et al²⁵, is based on two anatomical landmarks, the origin of the aorta and the apex of the heart. Currently, the two landmarks are manually provided by an expert. The aortic root is located inside the pericardium and forms the center of the heart coordinate system. This point is selected because it is easy to identify, the location has small variations, is located very close to the coronary artery ostia and inside the heart, which makes this landmark very suitable as a center location. To account for the geometry of the heart a spherical coordinate system is used. First, the voxel coordinates of the axial CT scans are transformed to the spherical space with an affine transformation. Then, the center of the coordinate system is transformed to the origin of the aorta by using a rigid transformation. Each heart scan is scaled by setting the radius equal to one, which corresponds to the distance from the two landmarks. Finally, the heart is in every scan aligned using two axes, find with anatomical landmarks, which reflect anatomical symmetry. Since the coronary arteries are usually located in the same respective regions of a heart. The HCC can now be used to align non-contrast CT heart volumes for the discrimination between coronary artery zones and their surrounding tissue.

Brunner et al published one of the first automatic methods for coronary calcium scoring²⁶. The authors used an unsupervised classification algorithm to distinguish between coronary artery calcifications and other calcifications in EBCT data. This is a feature based classification method, where the candidates are clustered. This method results in an average accuracy of approximately 80%. More recently, the same authors developed

an approach for automatic coronary calcium score with coronary artery region (CAR) models²⁴. First the HCC as described above is used to construct a family of CAR models for the detection of the main coronary arteries and their sub branches. With the HCC any coordinate point in scanner space is represented by its normalized heart centered coordinate (NHCC). These coordinates are used for representation of manually selected coronary artery trajectory points. Around these points a specific radius is applied, such that tube-like regions are created. Different radii are used because the diameter of the coronary arteries varies. Subsequently, the specific coronary artery zone and section radii are set. Nine coronary artery regions from three different zones are created, LM/LAD, LCX and RCA. Each coronary artery zone is divided into three distinct regions, proximal, mid, and distal. In the third step, the CAR models are trained using a support vector machine (SVM) framework with the trajectory point ground truth data to learn the extent of the nine coronary artery zones. The nine individual coronary artery regions and different radius settings for artery sections allows 16 different CAR models. Each individual CAR model is trained to detect coronary artery regions and areas outside the coronary arteries. Finally, a classification method is proposed that uses CAR models to automatically detect coronary calcium in the regions of the coronaries. First, candidate calcifications are detected. These are pixel areas of at least 1 mm² and a density of at least 130 HU. The coordinates of the candidates are transformed into the NHCC presentation. These coordinates are then used by the CAR models to train SVM classifiers using a Gaussian radial basis kernel function for the detection of coronary calcium. The CAR classifiers are able to detect coronary calcium with a mean sensitivity and specificity of 86.33 and 93.78% compared with a semi-automatic approach obtained by an expert. However, the results are limited, because it is only tested on 30 patients. Further studies with larger patient populations are required.

Another approach for automated detection of coronary calcium detection presented by Kurkure et al⁶. It is a supervised classification-based approach to distinguish the coronary calcifications from all the candidate lesions with a two-stage, hierarchical classifier. First, two sets of spatial features are used, the absolute location in the image coordinate system and the relative location in a HCC system. Subsequently, texture features are selected using the Laws texture energy measures. These are computed using convolution kernels generated from one-dimensional convolution kernels of five pixel length

characterizing level, edge, spot, wave and ripple patterns. An observer uses the candidate's regional properties instead of individual pixel properties to distinguish the coronary calcification from the rest. Based on this observation, features representing the neighboring regions of the calcifications are used to better discriminate between coronary calcium and the other structures. Additionally, object-related features are included. The feature selection is based on mutual information because when two features are inter-correlated, one of them can be removed without affecting the classification performance to reduce the computational load. Also, individually powerful features may not be so powerful together. A two-stage hierarchical classification-based method is used. In the first stage, it learns to distinguish the arterial calcifications from other highly dense regions present within the heart region. And in the second stage, another classifier is constructed using the features selected specifically to separate the coronary calcifications from the aortic calcifications. This is done because the negative class, with other high density structures, is broader and richer than the positive class, coronary calcifications. Training on such unbalanced classes will bias the classifier towards the majority class, and will degrade its performance. This problem is solved further by employing an asymmetric random sampling strategy. In asymmetric random sampling, the candidates are randomly selected from the majority class until the number of the selected candidates is equal to the number of the candidates from the minority class. The authors demonstrated that a two-stage hierarchical classifier using multiple classifiers is more robust in reducing the false positives while keeping a higher detection rate than the single stage classifiers. By using multiple classifiers for each stage of the hierarchy the accuracy improved. The individual classifiers decisions are combined to obtain the final decision. The best results are achieved by using the simple majority voting rule (MVR) for combining the multiple classifiers. This means that the final classifier uses the majority results of the multiple classifiers. The sensitivity and specificity of this approach are respectively 92.07 and 98.62%, in a testing dataset of 105 subjects. Instead of using the HCC by Brunner et al, a simple bounding box-based coordinate system is used to represent the location of the calcifications. By using the HCC of Brunner et al the results might improve.

Both methods are limited with respect to the imaging modality of EBCT due to poor spatial resolution. Another disadvantage is that the methods still require manual interaction. The method described by Brunner et al is almost fully

automatic, only the HCC requires manual seed points. With further improvements both methods could be very promising. Because of the limited studies of the CAR models, the two-stage hierarchical classification-based method of Kurkure et al is the preferred choice for calcium scoring with EBCT.

4.2 CT

For the automatic detection of calcium in the coronary arteries with CTA, a supervised classification-based approach is used by Isgum et al¹⁶. First, possible coronary calcifications are extracted using a threshold of 130 HU and component labeling. All objects bigger than 2500 voxels (1387 mm^3) are discarded as coronary calcifications and are not expected to have such a large volume. Subsequently, each object is represented by features describing its size, shape, location, intensity values, and variations of intensities within the object and their surroundings. For the spatial features, a HCC using a bounding box for segmentation of the aorta and heart is used. The segmentation of the heart is used to describe the object's location relative to it. The segmentation of the aorta is used to distinguish between coronary calcium and calcification in the aorta. The variation of intensities is based on image derivatives. These are computed by convolving the data with approximations of the derivatives of the Gaussian kernel. The method is tested with a direct classification and two stage classification in the same way as described earlier. There are also different classifiers tested with and without a feature selection scheme. The best performance is obtained employing a two-stage classification system with a k-nearest neighbor (k-NN) classifier and a feature selection scheme. The results show that feature selection is important for good performance of the system. Specially, the spatial features are very important. However, the aorta and heart segmentation do not give a satisfactory result. Segmentation of the aorta and heart is a difficult task, which is a disadvantage of this method. The size and shape features are less important, because they are not selected. The method uses 304 CT scans of one scanner and patients with age at menopause. 28 scans which did not give satisfactory results of the heart or aorta segmentation were excluded. This resulted in 200 training scans and 76 test scans. The outcome of the study is that the automatic method detected 73.8% of coronary calcifications at the expense of on average 0.1 false positives per scan. Also an evaluation with risk classification for the Agatston score as described in 2.4 is done. The method

assigned the correct risk category to 93.4% of the 76 scans.

To my knowledge, this is the first fully automatic method for automatic detecting calcium in the coronary arteries with MDCT. This method is used as a basis for other automatic methods. Specially, the spatial features are crucial for the identification of coronary calcium. If another method for extraction of the spatial features is used, for example the HCC describe by Brunner et al, the results might be improved. One other disadvantage of this approach is that the classifiers are trained on the unbalanced data. There are many negative candidates and therefore they are biased towards the majority class. This problem can be solved with the two-stage hierarchical classification-based method Kurkure et al used.

4.3 CTA

Several threshold-based approaches have been developed to derive the calcium score from CTA studies^{18,19}. A method to semi-automatically determine the calcium score, uses a fixed threshold of 320 HU and computed calcium scores by multiplying the calcium volume by a factor empirically derived from a training set of studies¹⁸. This threshold still detects lower density calcium, which may be found in early calcifications, but not non-calcified structures and small areas of contrast inclusion. A more promising method uses a dynamic threshold¹⁹. With a semi-automated scoring method the best threshold per patient is determined. This is very difficult, because the higher the threshold, more calcified plaques are missed and the detected lesions are smaller. The calculated CAC scores needs to be corrected depending on the applied HU threshold. Therefore a calibration factor, CF , was calculated using a linear regression analysis depending on the individual HU threshold from an initial cohort of 100 patients. The determined regression line showed a slope of -0.0003 and an intercept with the Y-axis at 0.4028. The Agatston score in CTA can be calculated with the following correction factor:

$$CF = \frac{1}{(\text{individual HU threshold} * \text{slope}) + Y - \text{axis}}$$

The accuracy of the developed approach is determined in 500 patients in comparison to CAC scoring in the CT. CAC scoring results in the CT and CTA scan showed a high correlation, $r = 0.954$ and with > 95% of the patients correctly assigned to the same risk group using the Agatston score. This study shows that calcium scoring in CTA is feasible and accurate. One disadvantage of using a threshold is that due to the partial volume effect,

calcium voxels that are closer to the vessel boundary are influenced more by the lower intensity tissues outside the vessel. In the scan this lesion is visible, but cannot be segmented by thresholding¹⁷.

For the automatic detection of coronary calcium in CTA there a lot of methods that use a coronary artery tree reconstruction^{27,17}. There are different methods to reconstruct a coronary artery tree^{28,29}, I will explain one of those methods^{29,30}. First, the lungs, mediastinum and aorta are detected and segmented. The lungs are detected as large areas filled with air and segmented using thresholding and morphological filters. The mediastinum is then detected as the area surrounded by the lungs and the aorta is detected and segmented using a 3D active surface minimization approach. The segmentation is used to create a mask of the aorta, which is used for detection of the ostia points. The ostia locations are detected via a vessel centerline extraction method which tracks the center axis of the coronaries starting from the aorta surface. Subsequently, a vessel enhancing filter is applied to the mediastinum volume image. Voxels with high filter response are combined into connected tubular components. The whole coronary tree is built by tracking tubular components using the depth-first-search (DFS) approach, while geometrical contiguous segments are connected. The four main coronary arteries (LM, LAD, LCX, and RCA) are labeled using a probabilistic anatomical model.

An algorithm for vessel segmentation that is capable of dynamically determining calcium plaques in CTA scans using vessel centerline extraction is developed by Wesarg et al³¹. A corkscrew algorithm for segmentation of the vessels is used. This is a path search algorithm, a connection is searched between the user-defined start and end point following a helical- or corkscrew-shaped path. A B-spline interpolation between the centers-of-gravity for each three subsequent sample points are the first estimation for the centerline, which is afterwards iteratively corrected by detecting the voxels belonging to the vessel border. Secondly, a vessel extraction approach is employed to exclude calcifications from the segmentation result. An additional three-step analysis based on the diameter function and the image data is performed because calcified regions are expected to lower the mean diameter and are 20-30% brighter than the vessel lumen that is filled with a contrast agent. The approach has an FP value of 0 tested with data of 10 patients. However, the segmentation does not always extract the whole artery because imaging

artifacts and the handling of bifurcations. This method did not segment the detected calcium and there is no calcium score calculated. Nonetheless, this method is important for automatic calcium score in CTA scans because it shows that automatic detection of calcium in CTA is possible and can be used as a basis for other more promising methods.

Teßmann et al²⁷ developed an automatic threshold-based method using a fully automatic segmented coronary artery tree. In order to deal with the high contrast variability on CTA data an individually threshold for each dataset is computed. For a correct threshold, a histogram, $H(x)$ based on the intensity values of the voxels along the automatically segmented vessel centerlines is generated. For using different datasets, the histogram values have to be normalized with respect to the number of entries, because the number of centerline points varies. If there are multiple maxima in the histogram, it is important to select the last significant peak for the threshold value because the HU value for calcified lesions lie above the HU values found for the contrast agent. Then, a smoothing step is applied to the histogram to get rid of noise and discontinuity. Subsequently, the histogram function is scanned for the last significant maximum number of hits. This is done so that the ideal HU threshold for calcified plaque segmentation corresponds to the lowest intensity value that belongs to calcium but does not fall into the range of contrast agent. In order to find the optimal threshold, the point where the descent from the peak positions flattens in the histogram has to be found. This is done by computing the derivative of the histogram and examining its values starting at the peak position until it exceeds a threshold. Voxels within a spherical radius of 1.5-2 mm of the centerlines of the coronary tree are examined. If the HU value is above the calculated threshold, it is marked as a possible candidate. The candidate points together with the threshold are then used as input seeds for a standard region growing algorithm. The resulting segmentation mask is used to identify single lesions and remove lesions whose size is below a certain value, to remove noise and flooding. Finally, the region growing process is repeated using the final marker list. The calcium score is evaluated by the segmentation results with the Agatston, volume and mass score. For the Agatston score a correction factor compensating for the different slice thickness in CTA is used. The exact value of this correction factor is unclear. The results show that the automatic thresholds are very close to those that are manually selected with a mean absolute distance of 72 HU and a standard

deviation of ± 73.59 . In 62% of the examined cases, the automatically detected segmentation threshold is lower than the segmentation threshold selected by the radiologist. But because flooding did not occur during region growing, there are more voxels that belong to a segmented calcified lesion, which increase the calcium score. Therefore, the authors conclude that most manually determined thresholds are too high. The ground truth score is created with a region growing based segmentation for the manual determined calcium. The resulting segmentation masks are used to generate ground-truth reference calcium scores. The correlation between ground-truth and automatic calcium score in 53 CTA is for the Agatston, mass and volume score 0.946, 0.951 and 0.950. Patients with cardiac motion are excluded from the study, which makes the results less accurate. This is a threshold based method, which means that the problem of detection small calcified lesions still remains. The resulted threshold is also compared with the manual selected threshold. However, finding a manual threshold in CTA is very hard. Therefore, for further research the results need to be compared with manual determined calcium scores on CT data. Nonetheless, using threshold-based techniques in CTA data will probably not give satisfying results.

An approach that can solve the problem of threshold-based techniques is a model-based segmentation approach, recently published by Eilert et al¹⁷. This method also makes use of a coronary tree represented by its centerlines and a list of coronary segments with detected external boundaries. The coronary segments are re-sampled along its centerline using the straightened curved planar reformation (CPR) and the external boundary is used as a surface in the straightened CPR coordinate system. The mean (μ_c) and the standard deviation (σ_c) of contrast material intensity levels inside the aorta are computed. An algorithm based on fitting an adaptive intensity distribution model to vessel intensity profile for every cross section along the vessel is used. The model describes the intensity profile of the given vessel as it would look if it has no calcium. To do that, the authors use a weighting function preferring vessel pixels that are more likely to represent contrast material, while ignoring areas that represent plaques. The following observations can be found using this model. Pixels above 150 HU and below $\mu_c + 3 \sigma_c$ are likely to be contrast material. Pixels below 50 HU are likely to be non-calcified plaque, thrombus or other tissue outside vessel boundaries and pixels above $\mu_c + 7 \sigma_c$ are very unlikely to be contrast material. The threshold

of 150 HU is the minimal mean intensity over 2300 CTA studies and the second threshold was calculated by the first threshold, $150 - 3\sigma$ aorta, which is ≈ 50 HU. Next, a parabolic model centered at the vessel centerline is used to describe the vessel cross-section intensity profile. The parabolic is < 0 , since the contrast intensity is higher than that of surrounding tissues. It is expected that the parabolic curvature, is larger for narrow vessels and smaller for wide ones. This is because the central part of a large vessel is almost not influenced by the partial volume effect. The presence of calcium can result in a wrong estimation of model parameters despite the used weighting factor. To deal with this problem, the parabolic has to be $> g(s)$. g is a negative, non-decreasing function of vessel cross-section found by analyzing parabolic models fitted to 30 healthy vessels of various sizes and fitting a quadratic lower bound to the parabolic. For the 3D vessel modeling, the parabolic model is fitted to each vessel cross section independently. In order to reduce the local model fitting error, a filter inspired by the bilateral filter is used. The paraboloid model does not describe bifurcations in the vessel correctly. Therefore the locations and directions of bifurcations are detected from the reconstructed coronary artery tree. In the segments affected by bifurcations, the parabolic intensity model assigns the parabolic peak value to all pixels affected by the bifurcation. With the vessel intensity model, a calcium binary map, M is generated by thresholding the difference between the actual image intensities, I and the values predicted by the model, \hat{I} . The threshold is set to 3σ , proportional to the image noise. The pixel intensity need to be higher than $\mu_c - \sigma$ to call it calcium. So, for every pixel (p):

$$M(p) = 1 \text{ if } |I(p) - \hat{I}(p)| > 3\sigma \wedge I(p) > \mu_c - \sigma$$

Otherwise, $M(p)$ is 0. The binary map is back-projected to the axial image volume to form the calcium binary mask. To calculate the calcium score from calcium binary mask, the standard calcium score on CT image is first simulated. To simulate the standard calcium score, a virtual CT image based on the CTA scan is build. First, the contrast of the CTA scan is virtually removed. Voxels that are brighter than blood > 40 HU which do not belong to the segmented coronary artery lesions are set to 40 HU. In this way other high density structures are also set to 40 HU, but this is no problem for the calcium score. Secondly, the image is resampled to the standard CT reconstruction. The degree of freedom in choosing the origin of the new 3 mm grid along the Z axis,

results in a different, but valid, calcium score. The Agatston score can now be calculated by applying the standard scoring function. In order to compensate for the calcium under segmentation, because of the low-intensity calcium voxels that can be recognized as contrast, still a calibration factor for the calcium score is used:

$$Ag = \sum_i S_i * \rho(S_i)$$

Where, i goes over all calcium lesions detected in the study. S_i is the initial score and $\rho(S_i)$ is the calibration factor of lesion i . The calibration factor is calculated with the ratio between the true and observed lesion volumes and the assuming that the calcium score is locally linear in lesion volume. The true lesion volume is from a calcium score study corresponding to the CTA data. The fully automatic system is tested in two independent clinical trials on 263 studies and demonstrates 0.95 and 0.91 correlations between calcium scores compared with manual CT score. Correspondingly, 211 out of 255 patients (82.7%) are categorized into the same risk group by both CT and CTA. The algorithm, used with the coronary tree, sometimes failed to track an artery beyond a total occlusion. The calcium lesion in the untracked distal part of the vessel is then undetected and not scored. This might not occur when a more complex coronary artery tree algorithm is used, although the algorithm that is used demonstrated very good results³⁰. The 2D intensity modeling might be improved by using local estimations of contrast intensity and noise level for calcium segmentation instead of the 3σ threshold. The authors also found that even if the calcium is detected and segmented perfectly there might occur some errors in the scoring. The model that is used for the calibration factor is limited on spherical lesions. A more complex model might reduce these scoring errors.

Calcium score on CTA is a very difficult task. The method by Wesarg et al shows that it is possible to detect coronary calcium in CTA but it is not able to calculate a calcium score. The results of the threshold based approach by Teßmann et al show a really high correlation between the manual and automatic method. Likewise, the model based approach, which also can detect the small calcium lesions, shows good results in coronary calcium score. The model based approach compares the results with manual CT calcium score instead of manual CTA score, which is a more accurate measurement. Therefore, the method presented by Eilert et al is better for automatic calcium scoring in CTA data. The results of the method by Eilert et al shows that it is possible to calculate the calcium

score automatically on CTA data in clinical practice. This means that the separate CT scan can be eliminated, which reduces the radiation exposure.

4.4 CT and CTA

The standard scanning protocol for plaque assessment consists of two scans: a native, low resolution CT and CTA. In the CTA, because of the contrast agent, the vessels are bright. By using both of these scans the location of the vessels in the CTA can be used for detection of the calcifications in the CT.

For detection of calcified coronary plaque a framework using CT and CTA is presented by Saur et al³². First the aorta is automatically detected³³ in the angio dataset and the coronary tree is segmented. For the coronary tree the rough estimate of the vessels centerline is obtained with a livewire algorithm³⁴. For this algorithm seed points need to be manually placed at the orifices of the coronary arteries and in the distal ends of the various branches. Each detected branch is reformatted along its centerline to get a stack of cross-sectional images. Graph cut is then applied to each cross-sectional slice using a circular shape prior. The resulting segmentation mask is then transformed back into the original angio data set. Plaque candidates are extracted using an intensity threshold from both the angio and the native data set. In the angio data set the coronary artery segmentation is used to only detect plaques inside the coronary arteries. For all possible plaque meshes are generated with the subsequent marching cube algorithm. This is a method for extracting isosurfaces from scalar volumetric data sets³⁵. For the Native Data Set (CT) a threshold of 130 HU is applied and candidates larger than 5000 mm³ are rejected. Using the same marching cube algorithm meshes of all plaques are generated. Each connected mesh is regarded as a native plaque candidate and is stored in a list. The same procedure is repeated but with a threshold of 200 HU, to generate a set of higher calcified native candidates. The native and angio data sets are generally not well registered due to the beating heart, breathing and minor patient movement. Therefore rigid plaque registration with Mevislab is performed. The registration uses the coronary segmentation results from the angio data on the native data set. This is done, so that the native candidates are limited to the segmented vessel regions. The registration also compares plaque features from both data sets with each other. To avoid misregistrations, only the very high calcified native plaques of 200 HU as well as the angio plaques with a volume $v > 5$ voxels are considered for registration. Furthermore, the native plaques

need to have an intensity score, s depending on its 90%-quantile intensity of its voxels that is > 0.95 to be considered. In the second stage of the registration, the mapping of angio-native pairs with the minimum energy is taken to compute the final registration rotation and translation parameters using the algorithm from Horn. The rotation and translation are then applied to all native candidates from 130 HU. Those candidates falling outside of the vessel boundaries after the registration are deleted from the list. In the end, a two rule based approach is used to maximize the number of detected plaques while minimizing false positives. First, several distance checks are applied to confirm the verified candidates resulting from the registration process and to search for additional pairs that were not considered by the registration process due to their low intensity. Secondly, angio candidates with its volume larger than 1 mm³ and $s \geq 0.75$ are added to the results. Because it is very likely that large angio plaque candidates with high intensity values are plaques even though a corresponding native candidate is missing. With the method weakly calcified plaques, hardly discriminable from the contrast agent in the angio data set, could be detected. The framework detects 86.3% of the 649 calcified plaques. The good performance of the proposed approach can be mainly attributed to the fusion of the native and angio data set. However, using rigid transformation only might not compensate for the movement of the heart between the different datasets. A rigid transformation followed by a non-rigid registration will probably work better for this registration task. By automatically labeling the segments of the coronary artery tree or using the coronary artery tree described in 4.3, the method could be fully automatic.

Shahzad et al³⁶ describes a method to automatically detect coronary calcium that uses a density estimate for the position of the main coronary arteries. From a training set of CTA datasets of 95 patients, a total of 10 CTA atlases were selected. For the atlases CTA datasets are used, because the contrast within these images gives a clear depiction of the heart chambers and the main coronary vessels. Lumen centerlines in the three main coronary arteries (LAD, LCX and RCA) were manually annotated in the remaining 85 CTA datasets. Each of the three manually annotated centerlines is transformed to each of the CTA atlases by non-rigid registration focused on aligning the entire heart and the chambers. Therefore, the mapped centerlines from the 85 scans are not overlapping but are spread over a region. This distribution gets sparser in the distal parts of the vessels. For the registration a multi-

stage registration approach using Elastix, a publicly available registration package, is used. First, for each resolution level 256 iterations of a stochastic gradient descent optimizer with the mean square difference (MSD) as cost function are applied. After that, the results of the affine registrations are used to initialize a B-spline registration. A stochastic gradient descent optimizer with 1024 iterations in each step is used with the Mutual Information (MI) as cost function. After the registration, the coronary density estimate for each voxel of the 85 atlases is determined for each of the three vessels separately in the following way. First for every voxel, the closest point with the Approximate Nearest Neighbors on each of the centerlines for each of the three main arteries is calculated. If this voxel is less than 10 mm away from the centerlines mean shift is applied, this is an iterative algorithm for locating the maxima of a density function. It calculates the mode of this particular voxel with respect to the 85 closest point set. The set of all locations that converge to the same mode defines the basin of attraction of that mode. These points are clustered based on their mode. Next, for each of the clusters the covariance of the points in that mode is determined. With this information the density estimate is calculated by summing the contributions of each of the clusters, where each cluster is represented by a multivariate Gaussian. This process is repeated for each of the voxels on the atlas image and separately for the three arteries. In the end, the obtained density estimates lying within the aorta were reset to zero. Because of anatomical variations between patients and inter-observer variation in the start point during annotation some of the mapped arteries lie partially in the aorta of the atlas and give thereby a high density estimate within the aorta. To do this, the aorta is automatic segmented using a multi-atlas based registration approach. In order to obtain patient specific coronary artery density estimation, the density fields obtained from the atlases are mapped onto either a CT or CTA image. This is done with a non-rigid registration of the atlas images to the CT or CTA images, transforming the density fields accordingly, and combining the density fields by averaging them. This coronary artery density estimate can then be used for fully automate calcium scoring. First, the intensity value of objects with an intensity > 130 HU and a volume > 1 ml were set to zero. This is done so that dense bony structures are not detected as coronary calcium. To avoid noise being detected as a false calcification, the connected components having a volume smaller than a certain value were removed. In the article the value of 0.02 ml is described. However, 0.02 ml is equal to 20 mm^2 which is a

very large area for noise, so this is probably a mistake. Subsequently, a ROI is obtained for the vessels by averaging the density fields from the 10 atlases. After that the CT image is limited at 130 HU to obtain all the calcifications. Finally, the automatic calcium scoring method on the CT dataset is evaluated with the Agatston score. The results show that the density estimates provide a reasonable estimate for the locations of the main arteries in both CTA and CT images. The automatically obtained Agatston scores for the 170 CT datasets are compared to the manually obtained Agatston scores. The authors only mentioned that the scores are linearly related to a Pearson regression coefficient R^2 of 0.88 and plotted the different scores. It is very hard to mutually compare the result of this method when the only result that is given is this coefficient. Nonetheless, the method shows that it is possible to derive calcium scores per vessel. Reporting the three calcium scores separately is expected to give better insights about the calcified plaque. The registration from the atlases to the patient scans often fails. Further research on this registration might improve the accuracy of the calcium scores. However, the used registration method looks already very promising for this task, so it is probably not possible to get a better registration. The results also might improve by using a wider set of atlases, covering more anatomical variations or by only using atlases that are most similar to the patient's anatomy. Furthermore, the calcium scoring results are different from the manual quantification. Using an appearance feature as described in 4.2, which could differentiate between a calcium spot and noise, the result might improve. This is done in a recently published method by the same authors.

Shahzad et al. use the density estimate as described above, for a feature-based classification approach³⁷. First, candidate calcium objects are determined from the CT scan by thresholding at 130 HU units and discarding all objects $> 1500 \text{ mm}^3$ and also those of $< 1.5 \text{ mm}^3$, which are assumed to correspond to respectively bone and noise. Subsequently, a classifier that uses local image features is applied to determine which of the detected candidate objects are coronary calcium. Two classifiers are built and trained, one for the 1.5-mm slice spacing data and one for the 3.0-mm data. In total, 62 features are considered. There are features describing the object size and shape. The intensity of the object at the maximum intensity point after Gaussian image derivatives is computed at five different scales for features describing the multi-scale image derivatives. The atlas-based density estimate is used for the

location estimate features. These features are used for the classification of candidate object and for assigning the calcifications to one of the main coronary arteries. For location features, the actual image space is registered with a standardized coordinate space. This is done by pairwise registration of the same 10 CTA atlas images as used for the density estimate. The registration consists of two stages, an initial affine registration followed by a non-rigid registration using ElastiX. The standardized space is then obtained by averaging the resulting deformations. The midpoint between the right and left coronary ostia is defined as the origin in the standardized space. The CT scan is then mapped into this standardized space. The resulting relative position is used for the location features. Subsequently, feature selection is performed to determine the set of features that gives optimal performance in detecting calcified objects in the coronary arteries. The authors found out that the best classifier for this problem is a k-NN classifier. The system calculates Agatston, mass, and volume scores for the detected calcium objects. Additionally, patients are assigned to the appropriate risk category using a model that also accounts for age and sex¹³. A completely automatic system that calculates calcium scores per vessel is then presented. Automatic detection of calcified objects is achieved with sensitivity and specificity of 81.2% and 99.6% per calcified per scan in the 1.5-mm data set and sensitivity and specificity 97.4% of 86.6% per calcified object in the 3.0-mm data set. Risk category assignment is correct in 95% and 89% of the data sets in the 1.5-mm and 3-mm scans. The authors conclude that the system slightly underestimates scores on 1.5-mm scans, while scores are slightly overestimated on 3.0-mm scans. However, the 1.5 data is tested on 101 datasets and the 3.0 data on 56 datasets and therefore the results are not directly comparable. The most errors in vessel labeling are caused by incorrect object classification and calcium objects are set to the wrong vessel. Per scan there are on average two misclassified objects. This problem can be solved, by using a CTA scan from the same patient but then there still will be two CT scans needed.

One disadvantage of the method by Saur et al is that it requires both a CTA and CT scan, which requires a high radiation dose. Both methods by Shahzad et al also make use of both scans. However, the CTA scans that are used are scans of a database. The manual centerlines are annotated offline and the atlas needs to be made only once for using it to calculate the density estimate per scan. As a result, these methods only require the CT scan from the patients and can also

be performed on CTA scans. However, there are no results for using these methods on CTA data. The features based classification method improves the detection of coronary calcium compared to using only the atlas based density estimate. Furthermore, the affine registration followed by a non-rigid registration used by Shahzad et al is probably more accurate than the rigid registration used by Saur et al. for the registration of the CT and CTA (or atlas) scan.

4.5 Chest CT

As described in 3.4, it is very promising to detect coronary calcium on chest CT screening data of heavy smokers. Recently, an automatic feature based method to detect coronary calcium in chest CT data is presented by Isgum et al¹⁴. This method is developed by the same authors as the featured based method described in 4.2¹⁶. The same indication of potential calcifications and features describing the size and texture are used here. Instead of using a HCC for the spatial features, the property that coronary calcification appear at typical locations in the scan is used. Therefore, a statistical map describing the typical locations and variations of the coronary calcification can be designed using multi-atlas based segmentation. An affine transformation followed by elastic registration is performed to calculate the derivative of mutual information using ElastiX. For the elastic registration, B-spline registration with four resolutions is used. With both registrations an iterative stochastic gradient descent optimizer with 512 iterations is used for the optimization of the cost function. The probabilistic map is then created by averaging the transformed binary segmentation of coronary calcifications. The map is blurred with Gaussian filter, to get a probabilistic estimation. The spatial features were then calculated using this coronary calcium map. With the same registration method each scan is registered to the calcium map. Nine spatial features are calculated, the candidate location in the atlas coordinate system, the probability a candidate is coronary calcium and the 3-D Euclidean distance of a candidate to the coronary calcium. Four supervised classifiers and three different classification strategies are evaluated. The three strategies are a single classifier classification, two-stage classification and a combination of the best performing classifiers. Also the importance of the features is evaluated. Experiments are done using all features, only features calculated with the coronary calcium map or only features calculated without the map. Finally, the method is evaluated with the volume score and the Agatston score for the cardiovascular risk as described in 2.3. The results are compared

with manual calcium scores obtained by two Radiologists. The best results are achieved with a combination of the best classifiers. These are the two-stage classification with k-NN classifier and SVM classifier, and single k-NN classifier with selected features. The sensitivity is on average 79.2% with the volume score tested on 231 scans of a multi scanner trial. The risk is correctly assigned in 190 of the 231 subjects (82.2%). Although results show that the spatial features are very important, the created coronary calcium map has a large region for the probability of coronary calcium. The authors think it is due to the difficult alignment of the coronary arteries in chest CT scans. Calcification in the aorta causes the largest FP errors. Segmentation of the aorta for spatial features might lead to a reduction in false positives. Furthermore, there has only been experiments with basic classifiers, more complex classifiers might also improve the results.

To my knowledge, this is the first fully automatic method for coronary calcium scoring using chest CT data. It would be beneficial to automatically detect coronary calcium in chest CT scans. The sensitivity of this automatic method is low compared to the automatic methods on other scan techniques. However, these results are limited due the scan technique. By using this method on CT data or make the atlas of CT data, the results probably improve.

5. Discussion

There are already several fully automatic and semi-automatic methods for the calcium scoring in CT data. An advantage of the fully automatic methods is that they do not depend on intra- and inter-observer variability. It is difficult to mutual compare the different automatic methods, because of the different scan techniques. Especially the automatic methods based on CTA need a very different approach compared with the other scan techniques. Although there are a lot of manual and automatic calcium scoring methods on CTA data, there is still not enough research that proves that the calcium score calculated on CTA data is accurate. However, the method of Eilot et al¹⁷ is very promising and shows that calculating a calcium score on CTA data is possible. The simple threshold based methods presented by Teßmann et al²⁷ might not give satisfying results compared to manual calcium score on CT data.

Although the methods that make use of EBCT by Brunner et al²⁴ and Kurkure et al⁶ seem promising, the data provided by EBCT is limited. In the current practice MDCT is used for the manual assessment of coronary calcium. Therefore, if the automatic methods become clinically, automatic

methods based on MDCT data are probably preferred. However, both of the methods on EBCT might also work on CT data and will probably give better results through the better spatial resolution of MDCT.

Another method that will probably give better results on CT data is presented by Isgum et al¹⁴ with chest CT data. However, by using chest CT data of screening trials for heavy smokers for the automatic calcium score it will be very interesting to identify patients who might benefit from preventive treatment. There should be more research on the coronary calcium map and registration of the coronary arteries in chest CT data to make this method more accurate.

The most automatic calcium score methods are based on the Agatston score. In clinical research the Agatston is a widely used scoring method and largely expected. However, as described before, the Agatston score is not always accurate and reproducible. This can lead to small variations in the results of the automatic calcium score methods. Some of the methods additionally use the volume and/or mass score to determine the calcium score. It is very hard to compare the different automatic methods with different calcium scores. If all automatic methods are calculated with the mass score method, which is more accurate and less variable then the Agatston or volume method, this will lead to more accurate and better comparable results.

Another limitation for mutual comparing the different automatic methods is the different test data. Some of the automatic methods make use of small numbers of data from one scanner. Isgum et al and Eilot et al make use of data from different protocols and scanners, which make the results more reliable compared with the other methods. A good cooperation step would be to develop a database per scan technique, to which the obtained accuracy for different calcium score methods should be reported. Furthermore, with studies of patients with low calcium score, the relative influence of small lesions is high¹⁷. This is because small lesions are easier to misinterpret. Therefore, it is important for the accuracy of the method to know it is tested on patients with all low calcium scores or all high calcium scores.

For further research, it would be interesting to combine some of the different methods to make the calcium score more accurate. Kurkure et al⁶, Shahzad et al³⁷ and Isgum et al¹⁴ all used a featured based classification approach. All show that this is a very promising approach for the automatic scoring of coronary calcium. For the spatial features, looking at the robust of the registration and the sensitivity to errors, the

density estimate presented by Shahzad et al, is my preferred choice. The coronary calcium map of Isgum et al will probably give almost the same results on CT data because the approach is to a certain extent similar. The results of those atlases might even improve by using atlases that are most similar to the patient's anatomy. Isgum et al and Kurkure et al showed that a combination of classifiers performed even better than the two-stage classification with K-NN classifiers. Using this for the method of Shahzad et al might improve these results even more.

Among the available methods for automatic calcium scoring, there are multiple methods that are very promising. With further research, for example combining different steps of the automatic methods and using more patient data, there are many possibilities to use automatic calcium scoring clinically. Specially, using automatic calcium scoring on chest CT data by screening trials for heavy smokers will be of high interest.

References

[Key Reference]

[Reference]

1. Budoff MJ, Shaw LJ, Liu ST, et al. Long-term prognosis associated with coronary calcification: observations from a registry of 25,253 patients. *J. Am. Coll. Cardiol.* 2007;49(18):1860–70.
2. Polonsky, T. S., McClelland, R. L., Jorgensen, N. W., Bild, D. E., Burke, G. L., Guerci, A. D., & Greenland, P. Coronary artery calcium score and risk classification for coronary heart disease prediction. *The journal of the American Medical Association.* 2010;303(16): 1610-1616.
3. Leschka S, Scheffel H, Desbiolles L, et al. Combining dual-source computed tomography coronary angiography and calcium scoring: added value for the assessment of coronary artery disease. *Heart.* 2008;94(9):1154–61.
4. Seitun, Sara, et al. "Calcium Score and Coronary Plaque." *Clinical Applications of Cardiac CT.* Springer Milan, 2012. 115-137.
5. Budoff MJ, Gul KM. Expert review on coronary calcium. *Vasc. Health Risk Manag.* 2008;4(2):315–24.
6. **Kurkure U, Chittajallu DR, Brunner G, Le YH, Kakadiaris I a. A supervised classification-based method for coronary calcium detection in non-contrast CT. *Int. J. Cardiovasc. Imaging.* 2010;26(7):817–828..**
7. Agatston, A. S., Janowitz, W. R., Hildner, F. J., Zusmer, N. R., Viamonte Jr, M., & Detrano, R. Quantification of coronary artery calcium using ultrafast computed tomography. *Journal of the American College of Cardiology.* 1990;15(4):827-832.
8. Callister T, Cooil B, Raya S. Coronary artery disease: improved reproducibility of calcium scoring with an electronbeam CT volumetric method. *Radiology.* 1998;(208):807 – 814.
9. Hong C, Becker C, Schoef U. Coronary artery calcium: absolute quantification in nonenhanced and contrast-enhanced multi – detector row CT studies. *Radiology.* 2002;(223):2474 – 480.
10. Budoff MJ, McClelland RL, Chung H, et al. Reproducibility of coronary artery calcified plaque with cardiac 64-MDCT: the Multi-Ethnic Study of Atherosclerosis. *AJR. Am. J. Roentgenol.* 2009;192(3):613–7.
11. Hoffmann U, Siebert U, Bull-Stewart A, et al. Evidence for lower variability of coronary artery calcium mineral mass measurements by multi-detector computed tomography in a community-based cohort—consequences for progression studies. *Eur. J. Radiol.* 2006;57(3):396–402.
12. Rumberger J a, Brundage BH, Rader DJ, Kondos G. Electron beam computed tomographic coronary calcium scanning: a review and guidelines for use in asymptomatic persons. *Mayo Clin. Proc.* 1999;74(3):243–52.
13. Hoff J a, Chomka E V, Krainik a J, Daviglius M, Rich S, Kondos GT. Age and gender distributions of coronary artery calcium detected by electron beam tomography in 35,246 adults. *Am. J. Cardiol.* 2001;87(12):1335–9.
14. **Işgum I, Prokop M, et al. Automated coronary calcium scoring in low-dose chest computed tomography. *Med. Phys.* 2012;31(12):2322-2334.**
15. Budoff MJ, Achenbach S, Blumenthal RS, et al. *Assessment of coronary artery disease by cardiac computed tomography: a scientific statement from the American Heart Association Committee on Cardiovascular Imaging and Intervention, Council on Cardiovascular Radiology and Intervention, and Committee on C.;* 2006:1761–91.
16. **Işgum I, Rutten A, Prokop M, van Ginneken B. Detection of coronary calcifications from computed tomography scans for automated risk assessment of coronary artery disease. *Med. Phys.* 2007;34(4):1450.**
17. **Eilott D, Goldenberg R. Fully automatic model-based calcium segmentation and scoring in coronary CT angiography. *Int. J. Comput. Assist. Radiol. Surg.* 2013.**

18. Otton JM, Lønborg JT, Boshell D, et al. A method for coronary artery calcium scoring using contrast-enhanced computed tomography. *J. Cardiovasc. Comput. Tomogr.* 2012;6(1):37–44.
19. Bischoff B, Kantert C, Meyer T, et al. **Cardiovascular risk assessment based on the quantification of coronary calcium in contrast-enhanced coronary computed tomography angiography.** *Eur. Heart J. Cardiovasc. Imaging.* 2012;13(6):468–75.
20. Henschke CI, Yip R, Farooqi AO, et al. Ordinal Scoring of Coronary Artery Calcifications on Low-Dose CT Scans of the Chest is Predictive of Death from Cardiovascular Disease. *Radiology*, 2010, 257.2: 541-548. 2010;257(2).
21. Budoff MJ, Nasir K, Kinney GL, et al. **Coronary artery and thoracic calcium on noncontrast thoracic CT scans: comparison of ungated and gated examinations in patients from the COPD Gene cohort.** *J. Cardiovasc. Comput. Tomogr.* 2011;5(2):113–8.
22. Wu M-T, Yang P, Huang Y-L, et al. Coronary arterial calcification on low-dose ungated MDCT for lung cancer screening: concordance study with dedicated cardiac CT. *AJR. Am. J. Roentgenol.* 2008;190(4):923–8.
23. Kim SM, Chung MJ, Lee KS, Choe YH, Yi C a, Choe B-K. Coronary calcium screening using low-dose lung cancer screening: effectiveness of MDCT with retrospective reconstruction. *AJR. Am. J. Roentgenol.* 2008;190(4):917–22.
24. Brunner G, Chittajallu DR, Kurkure U, Kakadiaris I a. **Toward the automatic detection of coronary artery calcification in non-contrast computed tomography data.** *Int. J. Cardiovasc. Imaging.* 2010;26(7):829–38.
25. Brunner G, Chittajallu DR, Kurkure U, Kakadiaris I. **A heart-centered coordinate system for the detection of coronary artery zones in non-contrast computed tomography data.** *Proc. Medical Image Computing and Computer-Assisted Intervention Workshop on Computer Vision for Intravascular and Intracardiac Imaging.* 2008.
26. Brunner G, Kurkure U, Chittajallu D, Yalamanchil R, Kakadiaris I, Toward unsupervised classification of calcified arterial lesions, In: *MICCAI* 2008; 5241(1): 144-152
27. Teßmann M, Vega-Higuera F, Bischoff B, Hausleiter J, Greiner G. **Automatic detection and quantification of coronary calcium on 3D CT angiography data.** *Comput. Sci. - Res. Dev.* 2010;26(1-2):117–124.
28. Gülsün MA, Tek H. Robust vessel tree modeling. *Med. Image Comput. Comput. Assist. Interv.* 2008;11(Pt 1):602–11.
39. Begelman G, Goldenberg R, Il H. **Creating a blood vessel tree from image data.** *U.S. Patent No 7,983,459.* 2011;2(12).
30. Goldenberg R, Eilat D, Begelman G, Walach E, Ben-Ishai E, Peled N. Computer-aided simple triage (CAST) for coronary CT angiography (CCTA). *Int. J. Comput. Assist. Radiol. Surg.* 2012;7(6):819–27.
31. Wesarg S, Khan MF, Firlie E a. **Localizing calcifications in cardiac CT data sets using a new vessel segmentation approach.** *J. Digit. Imaging.* 2006;19(3):249–57.
32. Saur SC, Alkadhi H, Desbiolles L, Székely G, Cattin PC. **Automatic detection of calcified coronary plaques in computed tomography data sets.** *Med. Image Comput. Comput. Assist. Interv.* 2008;11(Pt 1):170–7.
33. Saur, Stefan C., et al. Automatic ascending aorta detection in CTA datasets. *Springer Berlin Heidelberg*, 2008. 323-327.
34. Barrett W a, Mortensen EN. Interactive live-wire boundary extraction. *Med. Image Anal.* 1997;1(4):331–41.
35. Newman TS, Yi H. A survey of the marching cubes algorithm. *Comput. Graph.* 2006;30(5):854–879.
36. SHAHZAD, R., et al. **A patient-specific coronary density estimate.** *Biomedical Imaging: From Nano to Macro.* 2010 IEEE International Symposium on. IEEE, 2010. p. 9-12.
37. Shahzad R, van Walsum T, Schaap M, et al. **Vessel specific coronary artery calcium scoring: an automatic system.** *Acad. Radiol.* 2013;20(1):1–9.